Simulation Study of the Grid-Connected Single-Phase Impedance-Sourced NPC Inverter with Different Control Methods

C. Roncero-Clemente[1], O. Husev[2], E. Romero-Cadaval[1], J. Zakis[2,3], D. Vinnikov[3], M.I. Milanés-Montero[1]

[1] Power Electrical and Electronic Systems (PE&ES), University of Extremadura, Badajoz (Spain)
[2] Department of Electrical Engineering, Tallinn University of Technology, Tallinn (Estonia)
[3] Institute of Industrial Electronics and Electronic Engineering, Riga Technical University, Riga (Latvia)

Abstract—**Focus is on three operation strategies for a grid-connected three-level neutral-point-clamped quasi impedance source inverter in a single-phase application. Each control scheme was implemented in the PSCAD/EMTDC simulation tool and underwent different tests, which involved some steps in the reference values and in the perturbations applied to the system. A comparison according to their responses was based on different criteria, such as rise time, settle time, overshoot and steady state error, in order to determine which would be more suitable for such application.**

I. INTRODUCTION

Shortage of fossil fuels and the necessity of reducing CO_2 emissions among other reasons have significantly grown the number of inverter-based distributed generator (DG) connected to the low-voltage distribution network. Many of them interact with renewable energy sources (RESs) such us photovoltaic (PV) modules (Fig. 1 shows the installation). For a long time, PV inverters' function was merely to inject power into the main grid with a unitary power factor as the control reference [1] but under new trends and policies for PV plants they are integrated as active and smart devices [2]-[3]. As a burning ambition, this current philosophy contributes to the change from the traditional and linear power systems to the smartgrid and microgrid [4] concepts. In this way, PV inverters would be able to contribute to the local voltage support, improve the power quality and give rise to flexibility and security of supply. Some of those new demands for inverters are power flow controls [5], voltage level restoration at the point of common coupling [5]-[6] (PCC), active filtering capabilities [7], integration with energy storage systems [8], and communications compatibilities.

Concurrently, innovative ideas in terms of inverter circuitries have emerged during the last years. Some of them seem quite suitable for PV applications because they can step up the DC input voltage in a single power conversion stage by means of the shoot-through switching states, known as Z-source inverter (ZSI) family and its derivations [9]-[11].
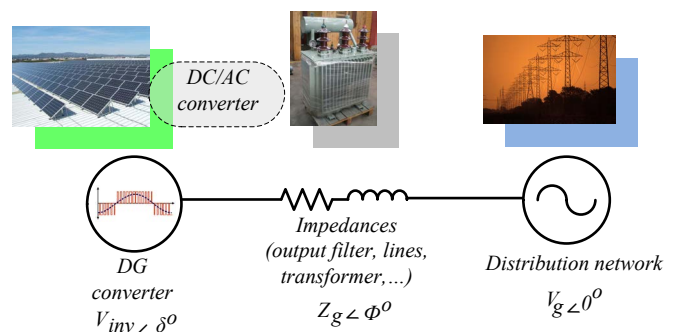

Fig. 1. Basic scheme of a grid-connected photovoltaic inverter.

Furthermore, ZSI family has been integrated with multilevel bridges to acquire their intrinsic advantages [12]. However, because of the relatively early stage, only few studies deal with the grid-connected integration with closed loop control systems, which basically must provide coexistence of an operation strategy of the inverter, a maximum power point tracking (MPPT), a DC-link voltage control method and a special modulation technique to embed the shoot-through states into the normal ones. For instance, a control strategy for the injected current in a grid-connected three-phase ZSI based on proportional-resonance and repetitive controllers is detailed in [13] in order to deliver a balanced set of current into a distorted system. A grid-connected three-phase PV quasi ZSI with a battery storage system is studied in [14]. The proposed control structure is based on a *d-q* rotational synchronous reference frame and a shoot-through control method to extract the maximum power for the PV array. A decoupling active and reactive power control is described in [15] for an application similar to that in [14].

In the particular case of grid-connected single-phase multilevel impedance family inverters (Fig. 2), some previous studies have dealt with the control system design [16]. As the original *d-q* and *p-q* theories were developed to three-phase three-wire or four-wire systems, they cannot be used directly for single-phase systems. Nevertheless, some approaches [17]-[18] to expand the three-phase *d-q* theory to single-phase systems can be found in the literature.

In section II, three different closed loop control systems with shoot-through regulation are proposed and schematically
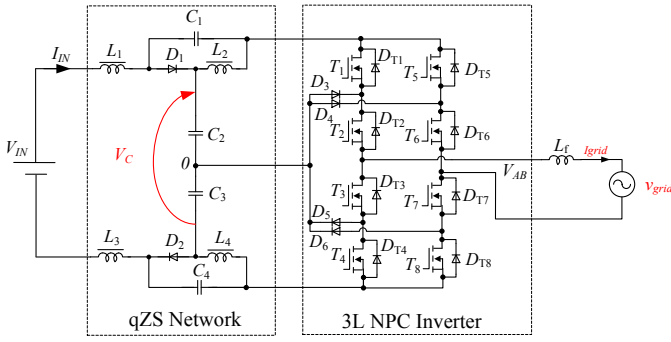
Fig. 2. Single phase 3L NPC qZS grid-connected inverter.

Fig. 3. a) Real and imaginary signals; b) $\alpha\beta$ to rotating d-q reference frame transformation.

explained for a single-phase three-level neutral-point-clamped qZSI (3L NPC qZSI) [19]. Next, the simulation study and the results obtained for each control structure are shown with emphasis on the system dynamics. Finally, different responses in each situation based on different criteria, such us rise time, overshoot and settling out to a steady state, are compared.

II. SCHEMES AND EXPLANATIONS OF THE PROPOSED CONTROL METHODS

In general, all inverter control strategies can be classified according to the controlled parameters: output voltage or current control, stationary or rotating reference frame and direct or indirect power control. In the PV inverter with intermediate boost, the DC-DC converter control system is divided as well. ZSIs are considered as single-stage converters, but with regard to the control system, they are considered as a two-stage structure due to the shoot-through duty cycle (D_S) with its additional control parameters.

Several approaches applied to grid-connected PV ZSIs are described in [20]-[24]. Their treatment in the shoot-through control is similar. By means of the MPPT block, the reference PV voltage (input voltage) is obtained. Taking into account that the capacitor voltage (V_C) remains constant, D_S is defined as [20]-[21]:

$$D_s = \frac{V_C - V_{IN}}{2V_C - V_{IN}}. \tag{1}$$

At the same time, voltage error on the capacitor (or DC-link) along with the PI controller are used for the power references. Stable capacitor voltage means balanced power between the demanded power from the PV panel and that injected to the grid. Usage grid voltage shape as reference shape for current provides only active power at the PCC. The main drawback of such approach lies in the low dynamic performance.

Another control strategy based on the d-q rotation frame, however different from those above, was proposed in [16] for a single-phase application. As mentioned earlier, based on the d-q theory, the three-phase system was developed, where the concept of orthogonal imaginary circuit was used. The main idea is to obtain two variables, the real one (measured voltage or current) and an imaginary one, with equal characteristics but
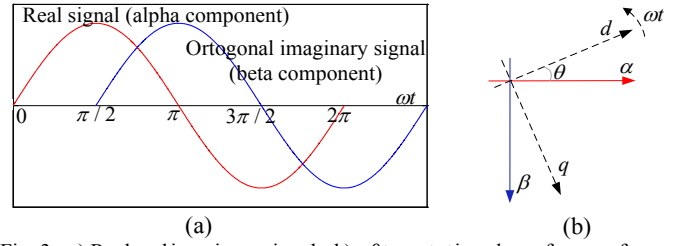
shifted 1/4 of the period of the real one. In this way, the measured signal is α component and the delayed signal is β component. This fact is illustrated in Fig. 3 a) and b). Shoot-through control strategy is different as well. D_s is regulated depending on the d and q components of the reference voltage ($V_{d,ref}$ and $V_{q,ref}$). The sketch of the grid side control shown in Fig. 4 a) is slightly modified as compared to that in [16].

According to this scheme, the control of active and reactive powers is carried out by two integral (I) regulators, which operate in a coupled way. Control action derived from the q current component error ($I_{q,ref}$-I_q) acts over the d and q component of the inverter reference voltage ($V_{d,ref}$ and $V_{q,ref}$). It means that this I controller adjusts the amplitude of the reference signal. Control action derived from the d current component error ($I_{d,ref}$-I_d) acts just over the q component $V_{q,ref}$, adjusting the phase of the inverter reference voltage. This reasoning is derived from the well known electrical relationships (between P-δ and Q-V). In addition, feedforward loops from the grid voltage are included to smooth the connection of the inverter to the grid, which avoids undesirable transients. Finally, as the d-q frame has the same frequency as the grid frequency, and the d axis is aligned with the grid voltage vector, the q component of the grid voltage will be zero [25].

When $V_{d,ref}$ and $V_{q,ref}$ are determined, the minimum value of the required DC-link voltage can be calculated. This reference value ($V_{c,ref}$) is compared with the measured DC-Link voltage (V_c) to activate or not to activate the $D_{s,ref}$, depending on whether the boosting voltage is needed or not, respectively. Shoot-through duty cycle is adjusted by the third I controller. Finally, the scaled reference signal as an input for the Sinusoidal Pulse Width Modulation (SPWM) block [19]-[25] is obtained:

$$v_{control} = \frac{(1 - D_{S,ref}) \, v_{ref}}{V_C}. \tag{2}$$

Fig. 4 b) shows a variant of the previous operation strategy by decoupling the active and reactive power control loops. In this proposal, control actions from ($I_{d,ref}$-I_d) and from ($I_{q,ref}$-I_q) are added to the $V_{d,grid}$ and $V_{q,grid}$ feedforward loops respectively, to generate the inverter reference signal. This approach is based on the following equations:

$$P = V_d I_d, \tag{3}$$

$$Q = -V_d I_q. \tag{4}$$

DC-link voltage control is exactly the same as in the previous case. Fig. 4 c) depicts a modification of the control strategy for the DC-link voltage control.
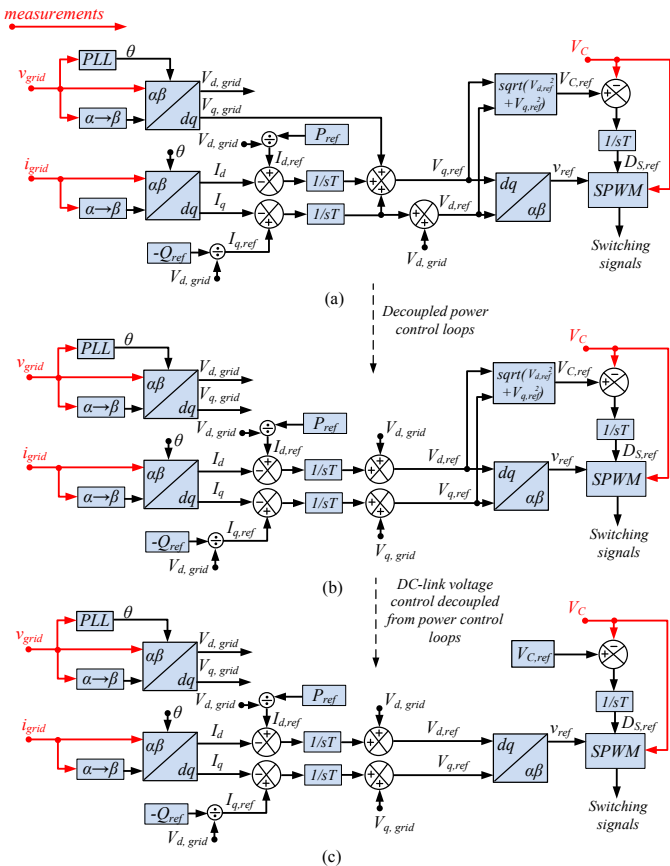

Fig. 4. Proposed control schemes: a) coupled power control loops and coupled DC-link voltage control; b) decoupled power control loops; c) decoupled DC-link voltage control.

In this case, this control loop is independent of the power controllers, and the DC-link voltage reference is given by a predefined value. In our case, this value ($V_{c,ref}$) is fixed at 350 V to assure the control of the injected current into the single-phase grid.

III. SIMULATION STUDY AND TRANSIENT RESPONSES

To validate and compare the three different control strategies described in section II, a comprehensive simulation study was performed in the PSCAD/EMTDC tool. The values of the passive elements of the qZ network and the output filter of the single-phase 3L-NPC qZSI were calculated according to the guidelines in [19] and [26].

The parameters for the PI controller were obtained similarly to [27] using the Ziegler-Nichols method based on the response curve [28]. All the different values and parameters used during the simulations are shown in Table I. As can be seen, the values of the PI controller are the same for all the proposed control schemes. The reason is in the same control object that mainly defines the dynamic behavior of the overall system.

As the main goal of this work is to analyze the system responses in dynamic conditions, different events were programmed. From the off-grid situation, the inverter is connected to the grid at second 0.2. Then, steps in $I_{d,ref}$ and $I_{q,ref}$ are implemented at seconds 0.5 and 1.2 respectively, in order to inject active and reactive power (2 A). Finally, the input voltage is suddenly reduced with a step as well, from 365 V to 295 V, because the boundary between the buck and the boost working mode is around 325 V (peak value of the grid voltage). With all these events it is possible to analyze all the control loops based on integral controllers.

TABLE I
VALUES FOR SIMULATION STUDY

Type	Simulation values			
	Parameter	Unit	Value	
Quasi-impedance network	Inductors $L_1, ..., L_4$	(mH)	0.29	
	Capacitor C_1, C_4	(mF)	4	
	Capacitor C_2, C_3	(mF)	1.3	
	Series resistance of L_i	(Ohm)	0.05	
Output filter	Inductor L_f	(mF)	2.2	
Grid impedance	Series resistance and inductance (R_g and L_g)	(Ω) (mF)	0.05	1.5
Electrical values	Input voltage V_{in}	(V)	365	
	Grid RMS voltage V_g	(V)	230	
Power controllers (scheme a)	Time constant for I_d	(s)	0.05	
	Time constant for I_q	(s)	0.05	
Power controllers (scheme b)	Time constant for I_d	(s)	0.05	
	Time constant for I_q	(s)	0.05	
Power controllers (scheme c)	Time constant for I_d	(s)	0.05	
	Time constant for I_q	(s)	0.05	
DC-link controller (scheme a)	Time constant for V_C	(s)	0.08	
DC-link controller (scheme b)	Time constant for V_C	(s)	0.08	
DC-link controller (scheme c)	Time constant for V_C	(s)	0.065	
Simulation parameters	Switching frequency	(kHz)	50	
	Simulation step	(μs)	0.25	

Different responses under described conditions are depicted in Fig. 5 a), b) and c). From top to bottom, the evolution of the grid injected currents (I_d and I_q components) for each control strategy is revealed.

Fig. 6 shows the evolution of different inverter parameters during the full simulation time. In a) the input voltage (green line) is represented, which is common in any developed simulation, allowing comparison under equal conditions. Capacitor voltage (V_c) is represented in the same picture (red line). Evolution of the shoot-through duty cycle is presented in b), and, c) and d) show the output voltages (V_{ab}) before filtering when D_s is zero and maximum, respectively.

Fig. 6 illustrates the control strategy presented in 4 b). For the other control schemes (Fig. a) and c)), waveforms are quite similar.

IV. COMPARISON AND DISCUSSION

Starting from the first event (inverter is connected to the grid), one can observe that it is produced at second 0.2. For each operation strategy, this process is really smooth (Fig. 5 a), b) and c)), mainly derived from the aforementioned grid voltage feedforward loops and well-tuned integral controllers (by means of the trial and error method). Those facts avoid undesirable transient currents on the inverter trip. From 0.2 to 0.4 s, the inverter is considered to be in a floating situation for all cases (P=0 and Q=0).
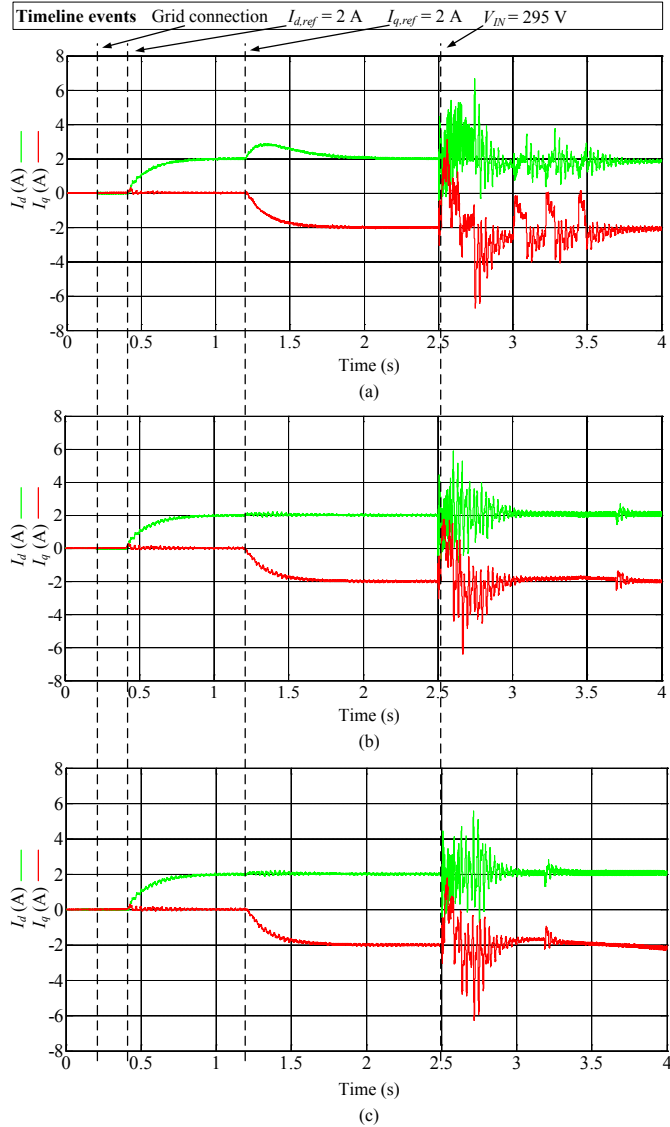

Fig.5. Responses of the system under programmed conditions: a) first control scheme; b) Second control scheme; c) third control scheme.

At second 0.4, a step in $I_{d,ref}$ is applied (From 0 A to 2 A) and this new reference is tracked with high accuracy by any control strategy (green lines in Fig. 5). In addition, it is possible to see that the influence on the I_q component is negligible (red lines). It is produced because the control actions in the direct component of the current act in one component of the inverter reference voltage.

At second 1.2 a new reference step is programmed in $I_{q,ref}$ (from 0 to -2 A). The new reference is tracked properly again in all cases but, for the first control strategy, it presents a coupling in the power loops. It is due to the control action over I_q error added to both components of the reference inverter voltage, in order to increase the modulation index of v_{ref}. This coupling is not presented for schemes b) and c), where merely one inverter component is affected by the current error.

Finally, at second 2.5 a perturbation in the input voltage (step from 365 V to 295 V) is applied. It will force the converter to change from the buck to the boost mode. In the case of the first control strategy, longer transients both to I_d and to I_q are observed before reaching again the steady state in both components. This undesired situation happens because the DC-link voltage control and power control loops are strongly coupled, therefore their influence is high. This transient is shorter in Fig. 5 b) and c) because of a lower coupling between the power control loops and between those ones and DC-link voltage control loop. In addition, a smaller ripple in I_d and I_q current components is observed in Fig. 5 b) and c) than in Fig. 5 a) at the end of the simulated time, which is also connected with the coupling between the control loops.

A quantitative comparison for each response presented in Table II is based on different parameters, such as rise time, overshoot, settling time, transient duration and steady state error. It will help to understand the previous discussion better.

Fig. 6 a) shows the input voltage (green line) and the capacitor voltage (red line) in the case of the control strategy in Fig. 4 b). When the input voltage step is applied, the converter changes from the buck to the boost mode and in this last situation, the capacitor voltage acquires the minimum required value to assure the desired active and reactive power. This situation also happens with the first control scheme but not with the last one, where a predefined $V_{c,ref}$ is given and obviously it will be greater than in the other controls.

TABLE II
RESPONSE PARAMETERS

| Type	Parameter	Unit	Loop I_d	Loop I_q	Loop V_c
Control scheme (frigure a)	Rise time	s	0.357	0.353	0.63
	Overshoot	%	0	0	0
	Settling time	s	0.6	0.581	1.271
	Steady state error	A	0	0	0
	Main features: 1) Strong coupling between power loops and between DC-link and power loops. 2) Minimum DC-link voltage.					
Control scheme (figure b)	Rise time	s	0.346	0.342	0.6
	Overshoot	%	0	0	0
	Settling time	s	0.5918	0.571	0.5
	Steady state error	A	0	0	0
	1) Insignificant coupling between power loops and strong between DC-link and power loops. 2) Minimum DC-link voltage.					
Control scheme (figure c)	Rise time	s	0.346	0.342	0.05
	Overshoot	%	0	0	0
	Settling time	s	0.5918	0.571	0.75
	Steady state error	A	0	0	0
	1) Insignificant coupling between power loops and strong between DC-link and power loops. 2) Not minimum DC-link voltage.					
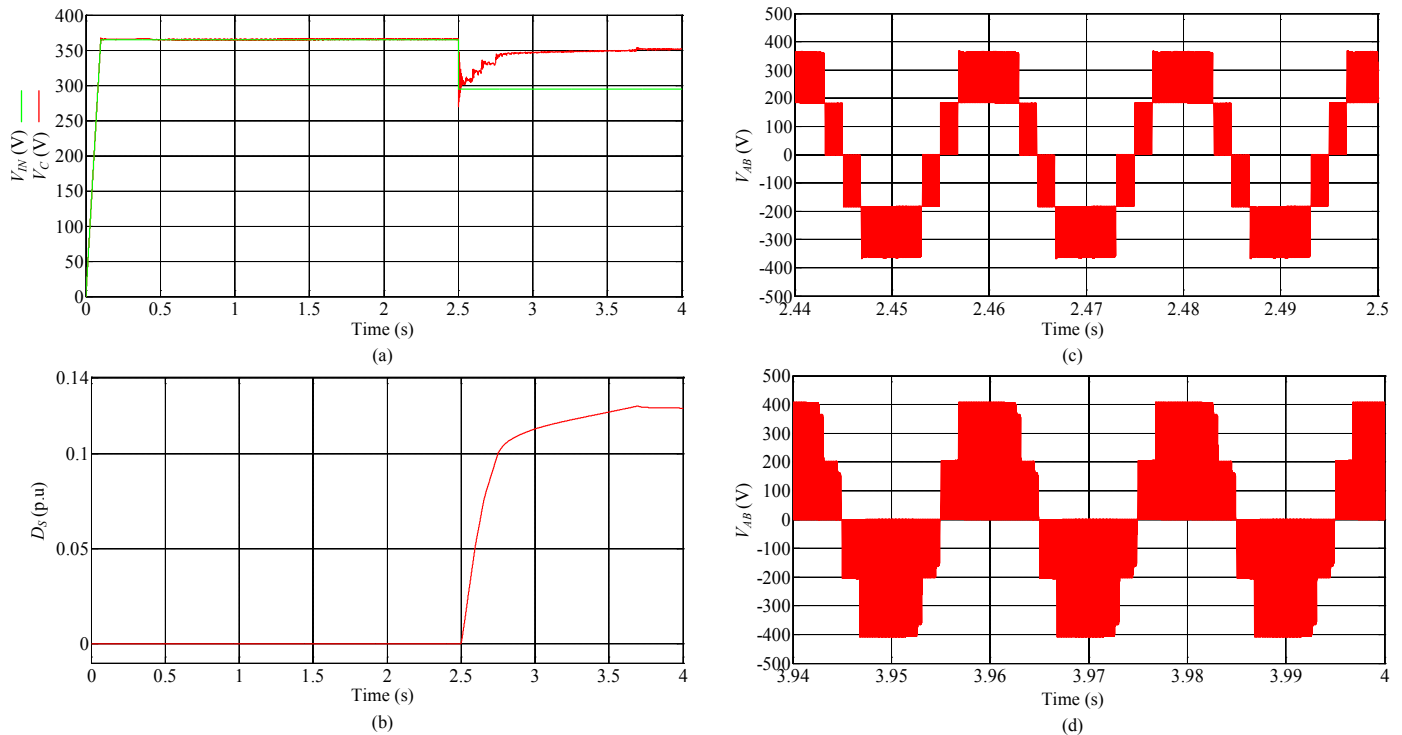
Fig. 6. Different magnitudes obtained with the second control scheme: a) input voltage (green line) and capacitor voltage (red line); b) shoot-through duty cycle; c) output voltage without shoot-through states; d) output voltage with shoot-through states.

The shoot-through duty cycle shown in Fig. 6 b) produces the aforementioned capacitor voltage evolution. The output inverter voltage under the shoot-through states illustrated in Fig. 6 d) (boost mode) is compared to that with the inverter working in the buck mode (Fig. 6 c). According to Fig. 6 a) and d), the maximum value of Vab is larger than that of Vc during the boost operation, since Vc matches with the average value of the DC-link voltage.

V. CONCLUSIONS

Different operation strategies for a single-phase 3L NPC qZS inverter for grid-connected applications have been proposed and compared in this paper. The control scheme shown in Fig. 4 a) demonstrates a strong coupling between its power control loops and between the DC-link voltage control loop. However, it works with a minimum value. Then, decoupled power control loops with a better dynamic response and the minimum value maintenance of the DC-link voltage were considered. Finally, in the last scheme, the DC-link control loop was found independent of the power control loops, in spite of the increasing the DC-link voltage level. All the control systems were tested in simulation under different dynamic conditions. Further research will focus on the converter and its control systems during transient events in the main grid and on the experimental validation of the ideas and conclusions derived from this work.

REFERENCES

[1] E. Romero-Cadaval, G. Spagnoulo, L. García-Franquelo, C. Ramos-Paja, T. Suntio and W. Xiao, "Grid-connected photovoltaic generation plants," IEEE Industrial Electronics Magazine, pp. 6-20. September 2013.

[2] K. Turitsyn, P. Sulc, S. Backhaus and M. Chertkov, "Options for control of reactive power by distributed photovoltaic generators," Proceeding of the IEEE, vol. 99, No. 6, pp. 1063-1073. June 2011.

[3] E. Romero-Cadaval, V. Miñambres-Marcos, A. Moreno-Muñoz, R. Real-Calvo, J. González de la Rosa and J. M. Sierra-Fernández, "Active functions implementation in smart inverters for distributed energy resources". IEEE Compatibility and Power Electronics CPE2013, 8th International Conference-Workshop. Conference proceeding, pp.52-57. Ljubljana (Slovenia), June 2013.

[4] J.M. Guerrero, J.C. Vasquez, J. Matas, L.G de Vicuña and M. Castilla, "Hierarchical Control of Droop-Controlled AC and DC Microgrids—A

General Approach Toward Standardization," IEEE Transactions on Industrial Electronics, , vol.58, no.1, pp.158,172, Jan. 2011.

[5] V. Miñambres-Marcos, M. A. Guerrero-Martínez, E. Romero-Cadaval, P. González-Castrillo, "Grid-connected photovoltaic power plants for helping node voltage regulation". IET Renewable Power Generation, 9 pp. DOI: 10.1049/iet-rpg.2014.0086. October 2014.

[6] J. Roldán-Pérez, A. García-Cerrada, J.L. Zamora-Macho, M. Ochoa-Giménez, "Helping all generations of photo-voltaic inverter ride-through voltage sags". IET Power Electronics, vol. 7, no. 10, pp. 2555-2563. October 2014.

[7] V. Minambres-Marcos, E. Romero-Cadaval, M.A. Guerrero-Martinez, M.I Milanes-Montero, "Three-phase single stage photovoltaic inverter with active filtering capabilities". 38th Annual IEEE Industrial Electronic Conference IECON 2012. Conference proceeding, pp.5253-5258. Oct. 2012.

[8] H. Beltrán, E. Bilbao, E. Belenguer, I. Etxeberria-Otadui and P. Rodriguez, "Evaluation of Storage Energy Requirements for Constant Production in PV Power Plants," IEEE Transactions on Industrial Electronics, vol. 60, no. 3, pp. 1225-1234 , 2013.

[9] F. Z. Peng, "Z-Source inverter", IEEE Trans. Ind. Appl. vol. 39, no. 2, pp.504-510, 2003.

[10] J. Anderson, F. Z. Peng, "Four quasi-Z-Source inverters," Power Electronics Specialists Conference, 2008. PESC 2008. IEEE , vol., no., pp.2743-2749, 15-19 June 2008.

[11] Y.P. Siwakoti, Fang Zheng Peng; F. Blaabjerg, Poh Chiang Loh; G.E. Town, "Impedance-Source Networks for Electric Power Conversion Part I: A Topological Review," IEEE Transactions on Power Electronics, vol.30, no.2, pp.699-716, Feb. 2015.

[12] L.G. Franquelo, J. Rodríguez, J.I. Leon, S. Kauro, R. Portillo, and M.A.M. Prats, "The age of multi-level converters arrives," IEEE Industrial Electronic Magazine, vol. 49, pp. 28-39, June 2008.

[13] C.J. Gajanayake, D.M. Vilathgamuwa, P.C. Loh, R. Teodorescu, F. Blaabjerg, "Z-Source-Inverter-Based Flexible Distributed Generation System Solution for Grid Power Quality Improvement," IEEE Transactions on Energy Conversion, vol.24, no.3, pp.695-704, Sept. 2009.

[14] Baoming Ge, H. Abu-Rub, F.Z. Peng, Qin Lei, A.T. Almeida, F.J. Ferreira, D. Sun; Y. Liu, "An Energy-Stored Quasi-Z-Source Inverter for Application to Photovoltaic Power System," IEEE Transactions on Industrial Electronics, vol.60, no.10, pp.4468-4481, Oct. 2013.

[15] Y. Liu; Baoming Ge, H. Abu-Rub, F.Z. Peng, "Control System Design of Battery-Assisted Quasi-Z-Source Inverter for Grid-Tie Photovoltaic Power Generation," IEEE Transactions on Sustainable Energy, vol.4, no.4, pp.994-1001, Oct. 2013.

[16] C. Roncero-Clemente, E. Romero-Cadaval, O. Husev, D. Vinnikov, "P and Q control strategy for single phase Z/qZ source inverter based on d-

q frame," IEEE 23rd International Symposium on Industrial Electronics (ISIE), pp.2048-2053, 1-4 June 2014.

[17] Y. Liu, J. Yang and Z. Wang, "A new approach for single-phase harmonic current detecting and its application in a hybrid active power filter", in Proc. Annu. Conference IEEE indust. Electron. Soc., (IECON'99), 1999, vol 2, pp. 849-854.

[18] V. Khadkikar, A. Chandra and B.N. Singh, "Generalized Single-Phase p-q Theory for Active Power Filtering: Simulation and DSP based Experimental Investigation", IET Power Electronics, vol. 2, no. I, pp. 67-78, January 2009.

[19] O. Husev, C. Roncero-Clemente, E. Romero-Cadaval, D. Vinnikov, S. Stepenko, "Single phase three-level neutral-point-clamped quasi-Z-source inverter ,"IET Power Electronics, vol. 8, issue 1, pp. 1-10. January 2015.

[20] M. Shahparasti, A. Sadeghi Larijani, A. Fatemi, A. Yazdian Varjani, M. Mohammadian, "Quasi Z-source Inverter for Photovoltaic System Connected to Single Phase AC Grid," 1 st Power Electronic & Drive Systems & Technologies Conference, IEEE , pp.456-460, 2010.

[21] Y. Li, J.G. Cintron-Rivera, F.Z. Peng, S. Jiang, "Controller Design for Quasi-Z-Source Inverter in Photovoltaic Systems," Energy Conversion Congress and Exposition (ECCE), 2010, IEEE , pp.3187-3194, 2010.

[22] S.M. Dehghan, E. Seifi, M. Mohamadian, R Gharehkhani, "Grid Connected DG Systems Based on Z-Source NPC Inverters," Power Electronics, Drive Systems and Technologies Conference (PEDSTC), 2011 2nd, pp.104-110, 2011.

[23] T.W. Chun, H.H. Lee, H.G. Kim, E.C. Nho, "Power Control for a PV Generation System Using a Single-Phase Grid-Connected Quasi ZSource Inverter," Power Electronics and ECCE Asia (ICPE & ECCE), 2011 IEEE 8th International Conference on, pp. 889 - 893, 2011.

[24] J.H. Park, H.G. Kim, E.C. Nho, T.W. Chun, "Power Conditioning System for a Grid Connected PV Power Generation Using a Quasi-Z-Source Inverter", Journal of Power Electronics, vol. 10, no. 1, pp. 79-84, 2012.

[25] P. Garcia-Gonzalez, A. Garcia-Cerrada, "Control system for a PWM-based STATCOM," IEEE Transactions on Power Delivery, vol. 15, no.4, pp.1252-1257, Oct 2000.

[26] O. Husev, A. Chub, E. Romero-Cadaval, C. Roncero-Clemente, D. Vinnikov, "Voltage distortion approach for output filter design for off-grid and grid-connected PWM Inverters". Journal of Power Electronics. Vol. 15, no.1, pp. 288-297, January 2015.

[27] C. Roncero-Clemente, O. Husev, S. Stepenko, D. Vinnikov, E. Romero-Cadaval, "Output voltage control system for a three-level neutral-point clamped quasi-Z-source inverter", Przegląd Elektrotechniczny, no. 5, pp. 76-80, May. 2013.

[28] C.C. Hang, K.J. Astrom, W.K. Ho, "Refinements of the Ziegler-Nichols tuning formula". IEEE Proceedings-D, vol.138, no.2, Mar. 1991.

2954